Title
Multimodality Imaging of β-Cells in Mouse Models of Type 1 and 2 Diabetes

Journal
Diabetes, 60(5)

ISSN
0012-1797

Authors
Yong, Jing
Rasooly, Julia
Dang, Hoa
et al.

Publication Date
2011-05-01

DOI
10.2337/db10-0907

Peer reviewed

Multimodality Imaging of β-Cells in Mouse Models of Type 1 and 2 Diabetes

Jing Yong,[1] Julia Rasooly,[2] Hoa Dang,[1] Yuxin Lu,[1] Blake Middleton,[1] Zesong Zhang,[1] Larry Hon,[1] Mohammad Namavari,[2] David B. Stout,[1] Mark A. Atkinson,[3] Jide Tian,[1] Sanjiv Sam Gambhir,[1,2] and Daniel L. Kaufman[1]

OBJECTIVE—β-Cells that express an imaging reporter have provided powerful tools for studying β-cell development, islet transplantation, and β-cell autoimmunity. To further expedite diabetes research, we generated transgenic C57BL/6 "MIP-TF" mice that have a mouse insulin promoter (MIP) driving the expression of a trifusion (TF) protein of three imaging reporters (luciferase/enhanced green fluorescent protein/HSV1-sr39 thymidine kinase) in their β-cells. This should enable the noninvasive imaging of β-cells by charge-coupled device (CCD) and micro-positron emission tomography (PET), as well as the identification of β-cells at the cellular level by fluorescent microscopy.

RESEARCH DESIGN AND METHODS—MIP-TF mouse β-cells were multimodality imaged in models of type 1 and type 2 diabetes.

RESULTS—MIP-TF mouse β-cells were readily identified in pancreatic tissue sections using fluorescent microscopy. We show that MIP-TF β-cells can be noninvasively imaged using microPET. There was a correlation between CCD and microPET signals from the pancreas region of individual mice. After low-dose streptozotocin administration to induce type 1 diabetes, we observed a progressive reduction in bioluminescence from the pancreas region before the appearance of hyperglycemia. Although there have been reports of hyperglycemia inducing proinsulin expression in extrapancreatic tissues, we did not observe bioluminescent signals from extrapancreatic tissues of diabetic MIP-TF mice. Because MIP-TF mouse β-cells express a viral thymidine kinase, ganciclovir treatment induced hyperglycemia, providing a new experimental model of type 1 diabetes. Mice fed a high-fat diet to model early type 2 diabetes displayed a progressive increase in their pancreatic bioluminescent signals, which were positively correlated with area under the curve–intraperitoneal glucose tolerance test (AUC-IPGTT).

CONCLUSIONS—MIP-TF mice provide a new tool for monitoring β-cells from the single cell level to noninvasive assessments of β-cells in models of type 1 diabetes and type 2 diabetes.
Diabetes **60:1383–1392, 2011**

From the [1]Department of Molecular and Medical Pharmacology, University of California, Los Angeles, Los Angeles, California; the [2]Departments of Radiology, Bioengineering, and Materials Science and Engineering, Molecular Imaging Program at Stanford, Stanford University School of Medicine, Stanford, California; and the [3]Departments of Pathology and Pediatrics, University of Florida, Gainesville, Florida.

Corresponding author: Daniel L. Kaufman, dkaufman@mednet.ucla.edu.

Received 30 June 2010 and accepted 7 February 2011.

DOI: 10.2337/db10-0907

This article contains Supplementary Data online at http://diabetes.diabetesjournals.org/lookup/suppl/doi:10.2337/db10-0907/-/DC1.

The expression of imaging reporter genes in β-cells has provided powerful tools for studying β-cell development, embryonic and adult stem cell differentiation into β-cells, transdifferentiation, and islet transplantation (1–13). Bioluminescent reporters, such as firefly luciferase, emit photons that can be detected with high sensitivity using a cooled charge-coupled device (CCD). We and others have demonstrated human and rodent islets can be genetically engineered ex vivo to express luciferase so that the islets can be monitored following their transplantation by CCD and that CCD signal corresponded with the implanted β-cell mass (1,2). Several laboratories have generated transgenic mice that express luciferase in their β-cells and shown that the CCD signal from the pancreas is correlated with β-cell mass (3–5). Moreover, the transgenic islets can be monitored after transplantation (3,4,6). Fluorescence imaging and bioluminescence imaging (BLI) are highly useful for research purposes in small animals, but they are not yet applicable to imaging internal organs in large animals because of the limited transparency of tissues to photons.

Positron emission tomography (PET) imaging is used clinically to assess various disorders of the heart and brain and for detecting various cancers (7,8). Islets that were engineered ex vivo to express a PET can be noninvasively monitored by microPET after implantation into the liver (9,10). The microPET signal reflects β-cell mass, and islets can be monitored long-term after implantation (11). Radiolabeled ligands of vesicular monoamine transporter (VMAT2) can image β-cells in BB rats, although VMAT2 may not be a sensitive biomarker of β-cell mass in humans (12–14). Mouse pancreatic β-cells are inherently difficult to detect by microPET because of the small size of mice, the long thin shape of the pancreas and its proximity to the probe excretion pathway—which eliminates the vast majority of the tracer and obscures the weaker signals from the pancreas, and the resolution of microPET (1–2 mm^3). Recent advances in PET reporter genes and PET probes with better clearance kinetics and biodistribution, however, have allowed progress towards microPET imaging of mouse β-cells in situ (14).

Previous imaging studies of β-cells have used animal models in which the β-cells express a single reporter gene. We have developed a series of trifusion imaging reporters consisting of a bioluminescent reporter (e.g., luciferase), linked by a few alanine residues to a fluorescent reporter gene (e.g., enhanced green fluorescent protein [*EGFP*]), which in turn is linked to a PET reporter (e.g., herpes simplex virus [HSV] thymidine kinase) (15). All three reporters are expressed as a single fusion protein, allowing

noninvasive CCD and PET imaging, as well as fluorescent microscopic analysis of tissue sections or fluorescence-activated cell sorter (FACS) isolation of single cells expressing EGFP (15,16). Using an insulin promoter to drive the expression of a trifusion reporter in transgenic mouse β-cells should enable the longitudinal monitoring of β-cells in the same mice by both CCD and microPET. After killing, fluorescent microscopy can identify β-cells at the cellular level and facilitate correlation of β-cell number and mass with the CCD and microPET signals. Because all three reporters are linked together in a fusion protein, the magnitude of signals from one imaging reporter should predict the magnitude of the signals from the other imaging reporters. Here, we provide proof-of principle of the utility of mice expressing a trifusion imaging reporter specifically in their β-cells in mouse models of type 1 diabetes and type 2 diabetes.

RESEARCH DESIGN AND METHODS

Animals. C57BL/6 MIP-TF mice were generated by injecting fertilized C57BL/6 oocytes with the MIP-TF DNA fragment described below. Founder mice were bred with C57BL/6 mice. We noticed some decline in the levels of pancreatic CCD signals with successive generations of MIP-TF mice. Therefore, we screened potential MIP-TF breeders or a few of their offspring for their pancreatic bioluminescent signal by CCD and used those with high pancreatic luciferase expression for breeding. This stabilized the pancreatic expression of luciferase at high levels in subsequent generations. Mice from line 300 were donated to the type 1 diabetes resource at The Jackson Laboratory (stock no. 12943 C57BL/6-Tg[Ins2-luc/EGFP/Tk]300Kauf/J). The MIP-TF transgene is also being bred into the NOD mouse background (stock no. 13116). FVB Tg(RIP-luc) mice were obtained from Xenogen (now Caliper Life Sciences, Alameda, CA) (3). MIP-GFP mice were generously provided by Manami Hara (17). All transgenic mice studied were heterozygotic for the transgene. All experimental protocols were approved by the University of California, Los Angeles Animal Research Committee.

Generation of MIP-TF transgenic mice. We previously constructed a series of different cDNAs encoding fusions of three imaging reporter proteins with different properties for bioluminescent, fluorescent, and PET imaging (15). We chose a trifusion cDNA construct containing the following: *1*) a mutant firefly luciferase gene, which was modified for higher enzymatic activity at 37°C and therefore enhanced bioluminescent imaging in vivo; *2*) EGFP because of its stronger fluorescent signal relative to GFP; and *3*) HSV1-sr39TK, which is modified for nuclear translocation and enhanced activity for PET probes (15). The trifusion cDNA was amplified using forward primer 5′-GCGCaacgttATG GAAGACGCCAAAAACAT-3′ containing an AclI site (restriction sites indicated by lower case) and reverse primer 5′-ACGCgtcgacCCGCATCCCCAGCATG CCTGC-3′ (containing a *Sal*I site), which is downstream of the trifusion cDNA stop codon and polyadenylation sequence. A 3.5-kb fragment containing the promoter region of the mouse insulin II gene (beginning 3.5 kb upstream of the ATG translational start signal and ending at this ATG) was amplified from 129/Sv mouse genomic DNA by PCR using forward primer 5′-CTGCatgcatAGG CTCCCATTCAGTCATTG-3′ (containing a NsiI site) and reverse primer 5′-GTCCatcgatggcgccggcCATGTTGAAACAATAACC-3′ (containing *Cla*I, NarI, NaeI sites). A region starting in insulin exon 2 and extending 3.6 kb 3′ downstream was PCR amplified using forward primer 5′-GCCGctcgagA AGCAGCACCTTTGTGGTTC-3′ (containing a *Xho*I site) and reverse primer 5′-GATCgacgtcTGACCTCTGCTGGACGCTTC-3′ (containing an AatII site). These PCR fragments were cloned sequentially into pNeoflox8 (removing the flox and Neomycin sequences) to generate pLARA-MIP-TF (Fig. 1*A*). In this construct, the trifusion cDNA (containing a stop and polyadenylation signal) is placed just downstream of the translational start signal of preproinsulin and then linked to 3.6 kb of downstream mouse insulin II genomic DNA, beginning within exon 2 to preserve any 3′ intron sequences that could contain transcription regulatory sequences. After amplification in transformed *Escherichia coli* the entire insert was excised, purified, and microinjected into C57BL/6 fertilized oocytes, which were then implanted into pseudopregnant C57BL/6 surrogate mothers. The resulting offspring were screened for the transgene by testing tail DNA for the presence of the *EGFP* gene (forward primer: 5′-AAATCGCTCCGGATACTGCG-3′ and reverse primer: 5-AGGGTTG GTACTAGCAACGC-3′). The transgenic lines were expanded by mating with wild-type C57BL/6 mice.

Diets. Mice were housed in microisolator caging and provided normal chow (Laboratory Research Diets, Catalog 5001). Where indicated, male mice (8 weeks old) were fed high-fat diet (HFD) containing 60% fat (Research Diets, D12492). Food and water were available ad libitum at all times except for a 14- to 16-h fasting period before intraperitoneal glucose tolerance test (IPGTT).

Bioluminescence imaging. Anesthetized mice were injected intraperitoneally with 126 mg/kg D-Luciferin (15 mg/mL in PBS). The mice were scanned using a CCD device (Caliper-IVIS; Caliper Life Sciences, Hopkinton, MA), as previously described (1). The firefly luciferase in the trifusion reporter has an emission of light centered on 560 nm, and the CCD camera has maximal quantum efficiency at 550–650 nm. Twelve consecutive bioluminescence images were obtained and analyzed using LIVING IMAGE 4 software (Caliper Life Sciences) with an acquisition time of 1 min for each frame. A photographic grayscale scale reference image was obtained under low-level illumination. To quantify emitted light, regions of interest were drawn over the pancreas region, and maximum photons/seconds/squared centimeters/steradian was determined. The data shown are the average of four maximum regions of interest values over the scanning period. Linear line graphs were plotted using Microsoft Excel 2003 software.

For bioluminescence imaging of isolated organs, mice were killed under anesthesia. Their pancreas, spleen, liver, kidney, lung, heart, brain, spinal cord, muscle, and skin tissues were quickly dissected out and placed in separate wells of a 16-well plate containing D-Luciferin (4.3 mg/mL) in PBS at 37°C. Bioluminescence images were taken with an acquisition time of 1 min and maximum bioluminescence in photons/seconds/squared centimeters/steradian was determined.

Luminescent bead imaging. A constant intensity luminescent bead (Mb-Microtec, Bern, Switzerland) was used to measure attenuation of pancreatic luminescence by overlaying tissue, as previously described (2,18). Three days after the final CCD scan, MIP-TF mice were killed and a small incision was immediately made on their ventral left side and a luminescent bead was inserted underneath the fat and above the pancreas head. The animal was imaged using an IVIS Lumina II imaging system (Caliper Life Sciences) with 1-s exposure. Attenuation was quantified by comparing the luminescence of the implanted bead versus the luminescence ex vivo of the bead. The slope of the linear regression relating the luminescence of the bead to mouse weight was used to normalize BLI measurements for mice fed a HFD.

Luciferase enzymatic activity assay. Luciferase activity was determined using a Luciferase Assay Kit (Stratagene). Briefly, pancreata of MIP-TF mice and control C57BL/6 mice were divided along their length (head to tail). One half was sonicated in 1 mL cell lysis buffer (Stratagene) for the luciferase activity assay, and the other half was immediately fixed in 4% paraformaldehyde (PFA) for histology. The homogenates were centrifuged at 15,000*g* for 15 min in a microcentrifuge. Protein concentrations in supernatants were determined using a Dc protein assay kit (Bio-Rad) and adjusted to 1 mg/mL. Luciferase activity was assayed in triplicate using 50 μL tissue homogenate with 100 μL assay buffer mixture in an opaque-walled 96-well plate (Corning) by a luminometer (Analyst HT).

Glucose tolerance test. To assess glucose tolerance, mice were fasted for 16 h and weighed. The mice were challenged with a glucose solution (2 mg/g i.p.), and their blood glucose levels were determined using a One Touch Ultra blood glucose monitor (Johnson and Johnson) 0, 15, 30, 60, 90, 120, and 150 min postinjection. Area under the curve (AUC) was calculated by the trapezoid rule for the glucose tolerance curve using Origin 6.0 software (Microsoft).

Streptozotocin, alloxan, and ganciclovir administration. A high dose of streptozotocin (STZ) (200 mg/kg) or a low dose of STZ (40 mg/kg i.p. five times) was used to ablate β-cells as indicated. Other mice were rendered diabetic by a low dose of alloxan (two administrations of 80 mg/kg i.v., 3 days apart) or administration of a low dose of ganciclovir (GCV; 50–75 mg/kg CYTOVENE-IV sodium salt [Roche Laboratories, Nutley, NJ]) through a subcutaneous minipump (Alzet) for 14 days. Diabetes onset was considered to be two consecutive blood glucose readings of >300 mg/dL.

Immunohistochemistry and pancreatic β-cell area determination. After fixation in 4% PFA overnight, pancreata were cryoprotected in 30% sucrose (in PBS) at 4°C until tissue sank to the bottom. Pancreata were then embedded in optimal cutting temperature compound and were sectioned into 5-μm thick slices. Slides were air-dried at room temperature for 30 min and stored at −20°C until use. Fixed pancreas sections were incubated with polyclonal anti-insulin from guinea pig (1:500; Cat. 18-0067; Zymed Laboratories), anti-somatostatin (1:500), or antiglucagon (1:500; Dako) followed by incubation with AF568 goat anti-guinea pig (insulin) or AF555 goat anti-rabbit (glucagon and somatostatin) secondary antibodies (Vector Laboratories). Negative controls included incubation with normal guinea pig or rabbit serum. Immunofluorescence was examined by an Olympus BX-60 microscope, and microscopic images were taken with a Macrofire camera mounted atop the microscope (Optronics; N = at least three mice/group). For fluorescence microscopy, the following wavelengths were used: Alexa-568; excitation-578 nm/emission-603 nm; EGFP excitation-489 nm/emission-508 nm; DAPI, excitation wavelength-360 nm/emission wavelength-460 nm.

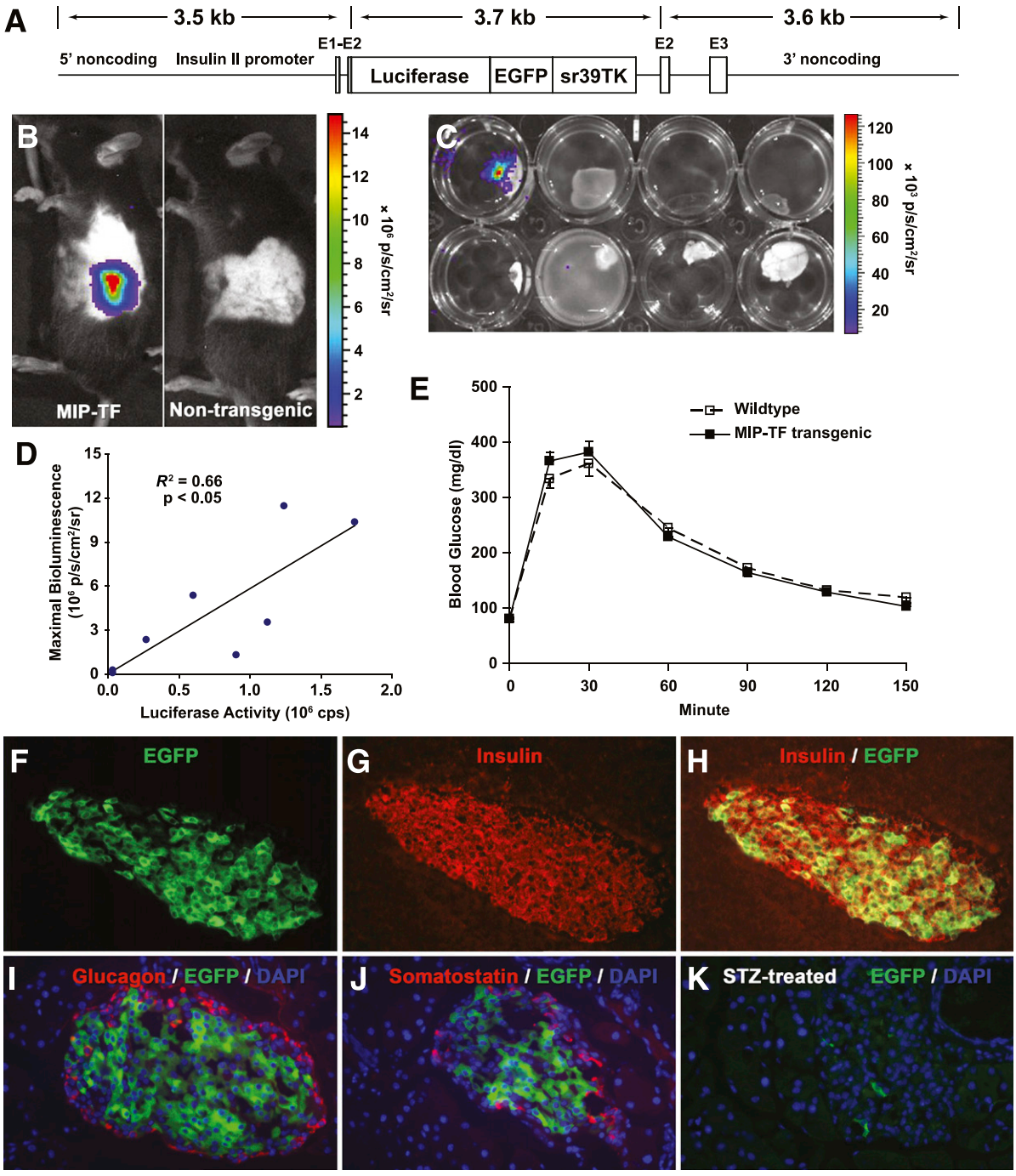

FIG. 1. Generation and characterization of MIP-TF mice. *A*: Diagrammatic representation of the construct used for microinjection. The trifusion reporter cDNA (firefly luciferase/EGFP/truncated HSV1-sr39TK) (15) is flanked on its 5′ end by 3.5 kb of genomic DNA upstream of the mouse insulin II ATG translational start site and, on its 3′ end, has 3.6 kb of genomic DNA that lies immediately 3′ of the ATG translational start site of insulin II. Exons of the insulin II gene are indicated as E1–3. *B*: Bioluminescence was detected specifically from the pancreas region of line 300 mice (referred to as MIP-TF mice; at *left*), but not a nontransgenic littermate (at *right*). The sides of both mice were shaved to maximize detection of bioluminescence. *C*: Representative BLI of freshly dissected organs from a MIP-TF mouse after luciferase injection. *Top row* (left to right): pancreas, liver, spleen, and heart; *bottom row* (left to right): lung, thymus, muscle, and brain. *D*: In vivo bioluminescence (measured as maximal radiance) showed a linear correlation with luciferase activity in pancreas homogenates ($R^2 = 0.66$, $P < 0.05$). *E*: IPGTT test. Data shown are the mean blood glucose levels after glucose challenge ± SEM; $n = 14$ mice/group. *F–H*: Expression of EGFP in β-cells of MIP-TF mice. Pancreas sections from MIP-TF mice were immunostained for insulin (red) and examined for EGFP expression (green) by fluorescence microscopy. Only insulin-positive cells also expressed EGFP. There was no overlap of EGFP expression (green) with glucagon (red; *I*), or somatostatin (*J*). Islets from mice rendered diabetic with STZ had few or no EGFP-expressing islet cells (*K*). (A high-quality color representation of this figure is available in the online issue.)

To determine pancreatic β-cell area, multiple pancreatic sections (separated by 50 μm) were stained with anti-insulin (by the 3,3′ diaminobenzidine color reaction), scanned using an Aperio ScanScope system, and then examined using Aperio ImageScope software. β-Cell area was defined as: insulin-positive area × 100/total pancreas tissue area (%). The average β-cell area (calculated by averaging three sections spaced by 100 μm at three different levels of the pancreas) for individual mice is shown, with four to six mice in each group.

MicroPET imaging, micro-computed tomography scanning, and microPET data analysis. These methods are detailed in Supplementary Data.

RESULTS

Generation and characterization of transgenic mice expressing a TF reporter gene. A genomic fragment, which extended 3.5 kb 5′ from the ATG translational start site (containing the promoter, exon 1, intron 1, and part of exon 2), of the mouse insulin II gene was subcloned 5′ of a TF cDNA containing a translational stop and polyadenylation signals on its 3′ end (Fig. 1*A*). To the 3′ end of the TF cDNA we linked the rest of the insulin II gene, beginning just after the ATG start site of insulin and extending 3.6 kb downstream (including the rest of exon 2, intron 2, exon 3, and additional noncoding region). The insulin II gene promoter was chosen because this gene is the predominant source for insulin synthesis in murine pancreatic β-cells (19). We injected the MIP-TF DNA cassette into fertilized C57BL/6 oocytes. Four founder transgenic mice were obtained (numbered 300, 324, 341, and 348), and each mouse line was expanded by mating with wild-type C57BL/6 mice. Their offspring were screened for the presence of *TF* gene by PCR. Transgene negative littermates were used as age-matched wild-type C57BL/6 controls.

Mice of line 324 had a strong bioluminescence signal from their pancreatic region, head, and spine (data not shown). Luciferase expression in the brain and spinal cord was verified by injecting the mice with D-Luciferin, dissecting out their major organs, and imaging the organs ex vivo with CCD. Histological analysis of their brains showed that luciferase expression occurred particularly in the choroid plexus. A previous study of mice with a β-galactosidase cDNA knocked into an insulin II gene observed expression of β-galactosidase in the β-cells and the choroid plexus of the brain (20). These observations, as well as others (19), support the notion that proinsulin may be expressed in the central nervous system. Mice from line 341 displayed weak bioluminescence signals from their pancreas region and from the ventral side of their necks (data not shown). The latter may reflect expression of proinsulin in the thymus, as described previously (19,21). Mice from lines 300 and 348 had bioluminescence signals exclusively from their pancreas region (mouse line 300 shown in Fig. 1*B*). The pancreatic BLI signals were higher from mouse line 300 than from line 348, so mouse line 300 was used for all subsequent studies. These mice are referred to hereafter as C57BL/6 MIP-TF mice. To verify the source of the bioluminescence, we injected MIP-TF mice with D-Luciferin, dissected out their pancreata, spleen, liver, kidney, lung, heart, brain, spinal cord, and muscle, and scanned them by CCD. As expected, only the pancreata emitted a bioluminescent signal (Fig. 1*C*), confirming that the reporter gene was exclusively expressed in the pancreas. After CCD imaging, pancreata from individual C57BL/6 MIP-TF mice were homogenized and assayed for luciferase enzymatic activity in vitro. The luciferase enzymatic activity showed a linear correlation with the magnitude of the pancreatic bioluminescent signal from individual animals ($P < 0.05$; Fig. 1*D*). There were no detectable bioluminescent signals or luciferase activity from wild-type mice or their dissected organs (data not shown). Importantly, age-matched MIP-TF and wild-type mice had similar responses to intraperitoneal glucose challenge (Fig. 1*E*), indicating that the transgene did not interfere with the β-cell response to a glucose challenge.

To examine the expression of the trifusion reporter at the cellular level, pancreas sections from MIP-TF mice were immunostained for insulin and examined for EGFP expression. Fluorescent microscopic analysis of pancreas tissue sections showed that EGFP expression was limited to cells that also expressed insulin (Fig. 1*F–H*). There was some variability in the EGFP intensity of fluorescence among islet β-cells, as has also been observed in other transgenic mice expressing imaging reporters in β-cells (3,6,22) and our own observations in pancreata from MIP-EGFP mice (17). There was no overlap of EGFP expression with glucagon (Fig. 1*I*) or somatostatin (Fig. 1*J*) expression. Islets from mice rendered diabetic by STZ administration had few, or no, cells that expressed EGFP (Fig. 1*K*). Thus the transgene is specifically expressed in MIP-TF mouse β-cells.

Evaluation of Tg(RIP-luc) mice. Concurrent with our studies of MIP-TF mice, we also characterized transgenic FVB/N mice that express luciferase (only) under the control of a rat insulin II promoter (Tg[RIP-luc mice]) (3,23), obtained from Xenogen (now Caliper Life Sciences). We found that the bioluminescent signals from their pancreas were about 20-fold less than that from MIP-TF mouse pancreas (Fig. 1*B* vs. Fig. 2). After Tg(RIP-luc) mice were given a high dose of STZ, the bioluminescent signal from their pancreas region rapidly declined, but a strong signal from their liver region arose a few days after STZ administration (Fig. 2), matching recent observations in these mice, which localized the transgene expression to occasional oval cells in their liver (23). We confirmed that the bioluminescence originated from the liver of diabetic Tg (RIP-luc) mice by CCD imaging isolated livers ex vivo (data not shown). Chan and colleagues (24) observed that hyperglycemia induces proinsulin expression in liver cells. However, we observed that some Tg(RIP-luc) mice given low doses of STZ or alloxan, which did not develop hyperglycemia, still had a rapid induction of a bioluminescent signal from their liver, although this signal was weaker than that following high-dose STZ administration. In contrast, neither high- nor low-dose STZ administration induced detectable transgene expression in MIP-EGFP (17) mouse livers (as measured by in vitro assay of liver homogenate fluorescence, data not shown) or in the liver of our MIP-TF mice (as measured by in vitro assays of fluorescence and luciferase activity in liver homogenates, data not shown) and by BLI of living MIP-TF mice as described below. The expression of luciferase in the liver of normoglycemic low-dose STZ and alloxan-induced Tg(RIP-luc)

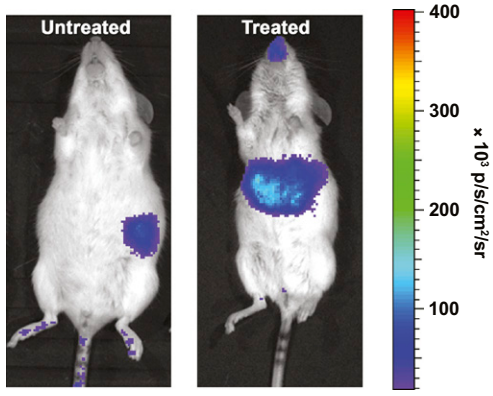

FIG. 2. STZ-induced expression of luciferase in the liver of Tg(RIP-luc) mice. Representative image of a Tg(RIP-luc) mouse before (at *left*) and 10 days after (at *right*) treatment with a high dose of STZ. The signal from the nose region of the mouse in the *right panel* is a reflection. (A high-quality color representation of this figure is available in the online issue.)

mice may result from the integration site of the transgene, the short rat insulin promoter (780 bp) used to drive luciferase expression, a response to transiently elevated glucose levels and/or toxin-induced oval cell stress. Notably, hepatotoxicity is known to activate oval cells, independent of hyperglycemia (25). We did not study the Tg(RIP-luc) mice further.

MicroPET imaging of MIP-TF mouse β-cells. The *TF* gene contains a modified thymidine kinase (HSV1-sr39TK) reporter gene optimized for microPET imaging (15). [^{18}F]FHBG has been widely used to image TK-expressing genes in tumor cells in mouse models. The MIP-TF mice were first imaged by BLI and then microPET scanned using [^{18}F]FHBG as a probe (Fig. 3). Six hours after probe injection,

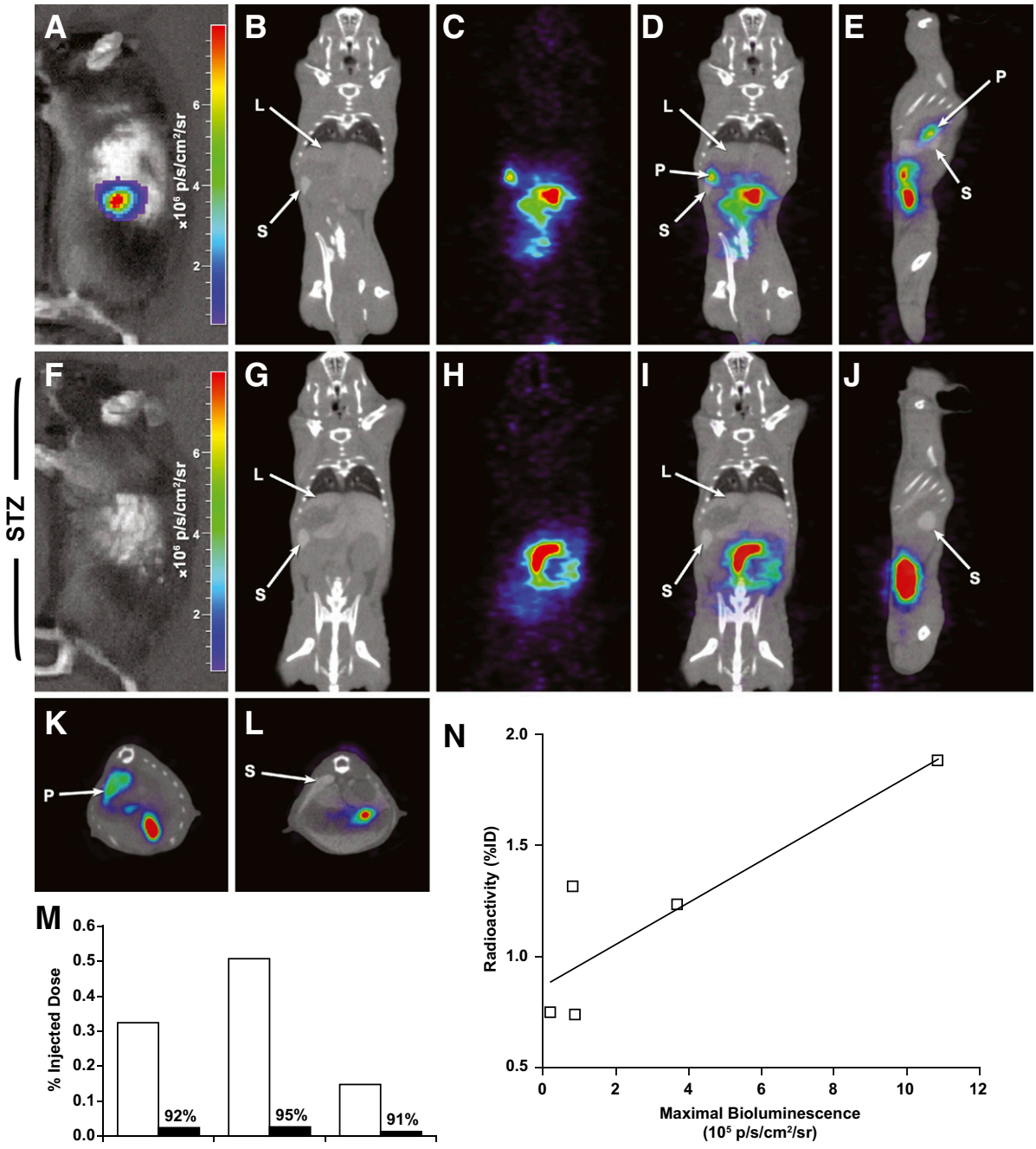

FIG. 3. MicroPET and CCD imaging of β-cells in MIP-TF mice. Representative CCD and microPET/CT images of a MIP-TF mouse before (*A–E* and *K*) and after (*F–J* and *L*) being rendered diabetic with STZ are shown. *A* and *F* show CCD images before, and after, STZ treatment, respectively. The same mouse was injected with [^{18}F]FHBG and imaged 6 h later with microPET/CT. Two hours before microPET, Fenestra was injected to provide spleen and liver contrast, so we could identify those organs in the CT images. *B–D*: Coronal CT scan (*B*), coronal microPET scan (*C*), and merged microPET/CT (*D*) before STZ treatment. *G–I*: Coronal CT scan (*G*), coronal microPET scan (*H*), and merged microPET/CT (*I*) after the mouse was rendered diabetic with STZ. *E* and *J*: Sagital microPET/CT images before and after STZ (respectively). *K* and *L*: Transverse microPET/CT images before and after STZ. "L" points to liver, "S" points to spleen, and "P" points to pancreas. Three mice were imaged before and after being rendered diabetic by STZ administration, and the change in [^{18}F]FHBG retention in the pancreas region of individual mice is shown (*M*). All microPET/CT images are on the same scale. In other experiments, the uptake of [^{18}F]FHBG in the pancreas region as measured by microPET imaging 5 h after probe injection was plotted against bioluminescence signal as measured by BLI for individual animals (*N*). A significant linear correlation (R^2 = 0.41) was found for [^{18}F]FHBG uptake and bioluminescence ($P < 0.05$). (A high-quality color representation of this figure is available in the online issue.)

signal from the pancreas region of MIP-TF mice was clearly discernable from other organs. Quantitative analysis of pancreatic [^{18}F]FHBG retention revealed that retained [^{18}F]FHBG radioactivity was significantly correlated with the magnitude of the bioluminescence signal from the same animal (Fig. 3*N*). After microPET imaging, some mice were rendered diabetic with STZ and then reimaged. Both CCD and microPET/computed tomography (CT) imaging showed that there was a great reduction in bioluminescence (Fig. 3*F*) and [^{18}F]FHBG retention (3G-M) from the pancreas region, confirming that these signals originate from β-cells. Thus MIP-TF mouse pancreatic β-cells can be detected by microPET, and there is an association between microPET and BLI signals, as has been observed in previous in vitro and in vivo studies using the trifusion reporter system in tumor models (15,16,26).

Using the low-dose STZ model of type 1 diabetes, pancreatic bioluminescence declines before the appearance of hyperglycemia. In an initial study, MIP-TF mice were given a high dose of STZ (200 mg/kg) or diluent. Pancreatic bioluminescence was measured by BLI before, as well as 3, 9, and 16 days after STZ injection. All STZ-induced diabetic mice (but not control diluent-treated mice) became highly hyperglycemic 3 days posttreatment, and their pancreatic bioluminescence dropped to baseline levels and remained so throughout the observation period (Fig. 4*A*). These data provide further evidence that *1*) the expression of the trifusion reporter gene is β-cell specific and *2*) β-cell loss in MIP-TF mice can be noninvasively monitored by BLI.

Next, we gave MIP-TF mice multiple low doses of STZ (40 mg/kg) for 5 consecutive days (as per [27]) and monitored their pancreatic bioluminescence longitudinally for 21 days. In this less rapidly progressing model of type 1 diabetes, we clearly detected loss of pancreas region bioluminescence before the appearance of hyperglycemia (Fig. 4*B*). The bioluminescent signals from the pancreas were reduced 2 and 4 days after STZ administration to an average of 63 and 54%, respectively, of the pretreatment level, during which time the animals remained normoglycemic. It was not until 10 days after beginning STZ administration that hyperglycemia became apparent, at which time the pancreatic bioluminescent signals had dropped to an average of 46% of its initial level. By the time the animals developed severe hyperglycemia, their pancreatic bioluminescent levels were on average only 8% of their initial levels. In contrast, a control group of MIP-TF mice

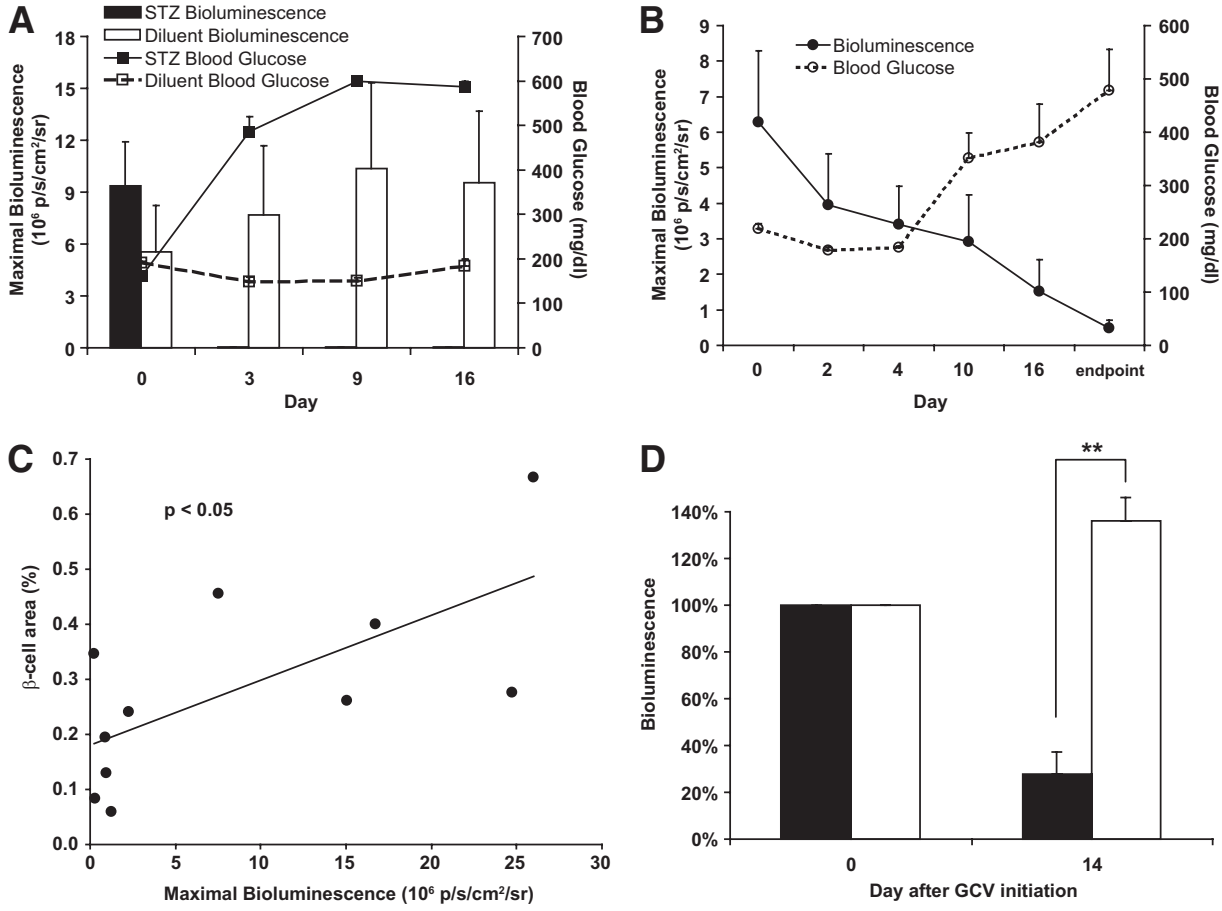

FIG. 4. CCD imaging of MIP-TF mice in type 1 diabetes models. *A*: Longitudinal monitoring of pancreas region bioluminescence and blood glucose levels in MIP-TF mice given a high dose of STZ administration (200 mg/kg i.p., once) or diluent. Data shown as bars are the mean maximum photons/seconds/squared centimeters/steradian ± SEM for MIP-TF mice given STZ (black bars) or diluent (white bars). Solid line indicates mean blood glucose level ± SEM for MIP-TF mice given STZ; dashed line is that for diluent-treated mice. After STZ administration, bioluminescence dropped >300-fold to baseline levels (n = 6 mice/group). *B*: Longitudinal monitoring of pancreas region bioluminescence and blood glucose levels in MIP-TF mice that developed hyperglycemia following multiple low doses of STZ (40 mg/kg i.p. for 5 consecutive days). Solid line indicates mean maximum photons/seconds/squared centimeters/steradian ± SEM; dashed line represents mean blood glucose levels ± SEM (n = 3 mice). *C*: Linear correlation between β-cell area and BLI for individual diluent or STZ-induced MIP-TF mice ($P < 0.05$). *D*: Correlation of pancreatic BLI with β-cell is from individual mice. *D*: Pancreatic region bioluminescence before and 14 days after control diluent (white bars) or GCV (black bars) treatment and the development of hyperglycemia in the latter. Data shown are change in mean bioluminescence (n = 3 mice/group). **$P < 0.01$.

that received citrate diluent injections maintained stable pancreatic bioluminescence and blood glucose (data not shown). After a last CCD scan, the mice were killed and we determined the islet β-cell area for individual STZ-induced and diluent-treated MIP-TF mice. We found a linear correlation between β-cell area and bioluminescent signal (Fig. 4*C*, $P < 0.05$).

Herpes simplex virus thymidine kinase with ganciclovir (GCV) is a widely used suicide gene/prodrug system. Because MIP-TF mice specifically express HSV1-sr39 thymidine kinase in their β-cells, treatment with GCV should ablate their β-cells, providing a new experimental model of type 1 diabetes. MIP-TF mice given a low dose of GCV developed hyperglycemia within 14 days of treatment at which time there was an average 72% reduction in the BLI signal from the pancreas region (Fig. 4*D*).

CCD monitoring HFD-induced changes in β-cell function. C57BL/6 mice fed a HFD are a widely used model of the early stages of type 2 diabetes (28–30). HFD-fed mice develop glucose intolerance, increase their β-cell mass, and progress to hyperglycemia. We examined whether monitoring luciferase expression in MIP-TF mice by BLI provides a surrogate marker of the increased insulin gene transcription during the early stages of type 2 diabetes development.

Eight-week-old MIP-TF mice were placed on a HFD or normal mouse chow, and their pancreatic bioluminescence and weight were monitored longitudinally over 60 days. Both normal chow and HFD-fed mice gained weight over this observation period, but mice fed the HFD diet gained weight at a faster rate (Fig. 5*A*). As expected, HFD feeding led to elevated fasting blood glucose (data not shown) and impaired glucose tolerance, as evidenced by significantly increased AUC-IPGTT at day 40 and day 60 compared with the control diet group (Fig. 5*B*). On days 10 and 20, the bioluminescent signals from mice fed a HFD were almost twofold higher than that of their littermates that were fed a normal diet (days 10 and 20; Fig. 5*A*). However, BLI measurements taken at later time points (days 40 and 60) showed that pancreatic bioluminescent signals from HFD and normal chow-fed mice were similar in magnitude. We surmised that with the progressive development of obesity, the increasing tissue overlying the pancreas blocked pancreatic bioluminescence to a greater extent in HFD-fed mice, as was previously observed in a study of HFD-fed transgenic mice that express luciferase in their β-cells (5). To discern the extent to which the pancreatic photonic signal was attenuated by the increased body mass of HFD-fed animals, the mice were killed a few days after the last CCD scan, and a fluorescent bead that emits constant amount of light was implanted above their pancreas and the mice were CCD imaged, as previously described (5,18). We found that light from the luminescent bead attenuated linearly with increasing mouse weight (Fig. 5*C*, $P < 0.01$). The average attenuation of light from the implanted bead in HFD-fed mice was approximately threefold more than that in control mice. After correction for this interference, the pancreatic bioluminescence for HFD-fed group at day 60 was actually 3.6-fold higher than that of control mice (Fig. 5*D*, $P < 0.05$ by two-tailed t test). Moreover, although uncorrected pancreatic bioluminescence did not correlate with AUC-IPGTT values at day 60, after correction for attenuation, bioluminescent signals were linearly correlated with AUC-IPGTT (Fig. 5*E*, $P < 0.01$). Finally, we excised the pancreas and determined pancreatic β-cell area in individual mice. There was a linear correlation between β-cell area and the magnitude of the last pancreatic bioluminescent signal from individual control and HFD-fed mice (Fig. 5*F*). These data suggest that monitoring *MIP-TF* gene expression (by BLI) provides a surrogate marker of pancreatic β-cell function and area.

DISCUSSION

We have generated transgenic mice in which pancreatic β-cells express a fusion protein of three different imaging reporters. Expression of the trifusion reporter transgene had no apparent effect on mouse weight, islet morphology, fasting blood glucose, or glucose tolerance. We demonstrated that MIP-TF mouse β-cells were readily identified in pancreatic tissue sections using fluorescence microscopy, as in previous studies of MIP-EGFP mice (17). Additionally, we showed that both BLI and microPET can noninvasively monitor MIP-TF mouse β-cells. Previous studies have generated transgenic mice expressing luciferase in their β-cells (3–5). The β-cells of MIP-TF mice have especially high levels of luciferase activity, perhaps because the trifusion cDNA expression is enhanced by the long stretches of the insulin II gene genomic DNA that surround it and/or because its luciferase has been modified for greater enzymatic activity at 37°C.

Using microPET/CT, we could clearly delineate preferential accumulation of [^{18}F]FHBG in the pancreas of MIP-TF mice. Noninvasive microPET imaging of mouse pancreatic β-cells is technically challenging because of the small size of mice relative to small animal PET scanner spatial resolution, the small size of their pancreas, and its proximity to tracer excretion pathways (9–11,14). Six hours postprobe injection, the vast majority of the probe had cleared through its excretion pathway, and there was sufficient probe retention in the pancreas such that the pancreas could be readily discerned from surrounding organs. After rendering mice diabetic by STZ administration, probe retention in the pancreas region was reduced by 91–95% in individual mice, confirming that the probe was originally retained by β-cells. The magnitude of pancreatic microPET signals showed a significant correlation with pancreatic bioluminescence from individual mice. Correlation between reporter proteins originating from the same fusion cDNA has been observed in previous in vitro and in vivo studies of tumors expressing linked reporter molecules (e.g., 15,16,26) and allows flexibility in the modalities used to monitor biological processes.

After administering a high dose of STZ, bioluminescent signals from the MIP-TF mice dropped to essentially background levels, proving to be further evidence that the expression of luciferase was β-cell specific. Using the more slowly progressing multiple low-dose STZ model of type 1 diabetes, we observed a progressive loss of pancreatic bioluminescent signals, which preceded the appearance of hyperglycemia. By the time the mice developed severe hyperglycemia, only 8% of the bioluminescent signal remained. The timing and magnitude of the changes in pancreatic bioluminescence correspond well with the gradual loss of β-cells previously described in C57BL/6 mice after administration with low-dose STZ (27,31). There was a linear correlation between β-cell area and bioluminescence for individual MIP-TF mice, suggesting that noninvasive monitoring of *MIP-TF* gene expression by BLI can provide a biomarker of endogenous β-cell mass. In addition, we show that treatment with GCV induces hyperglycemia concomitant with a large decrease in bioluminescence

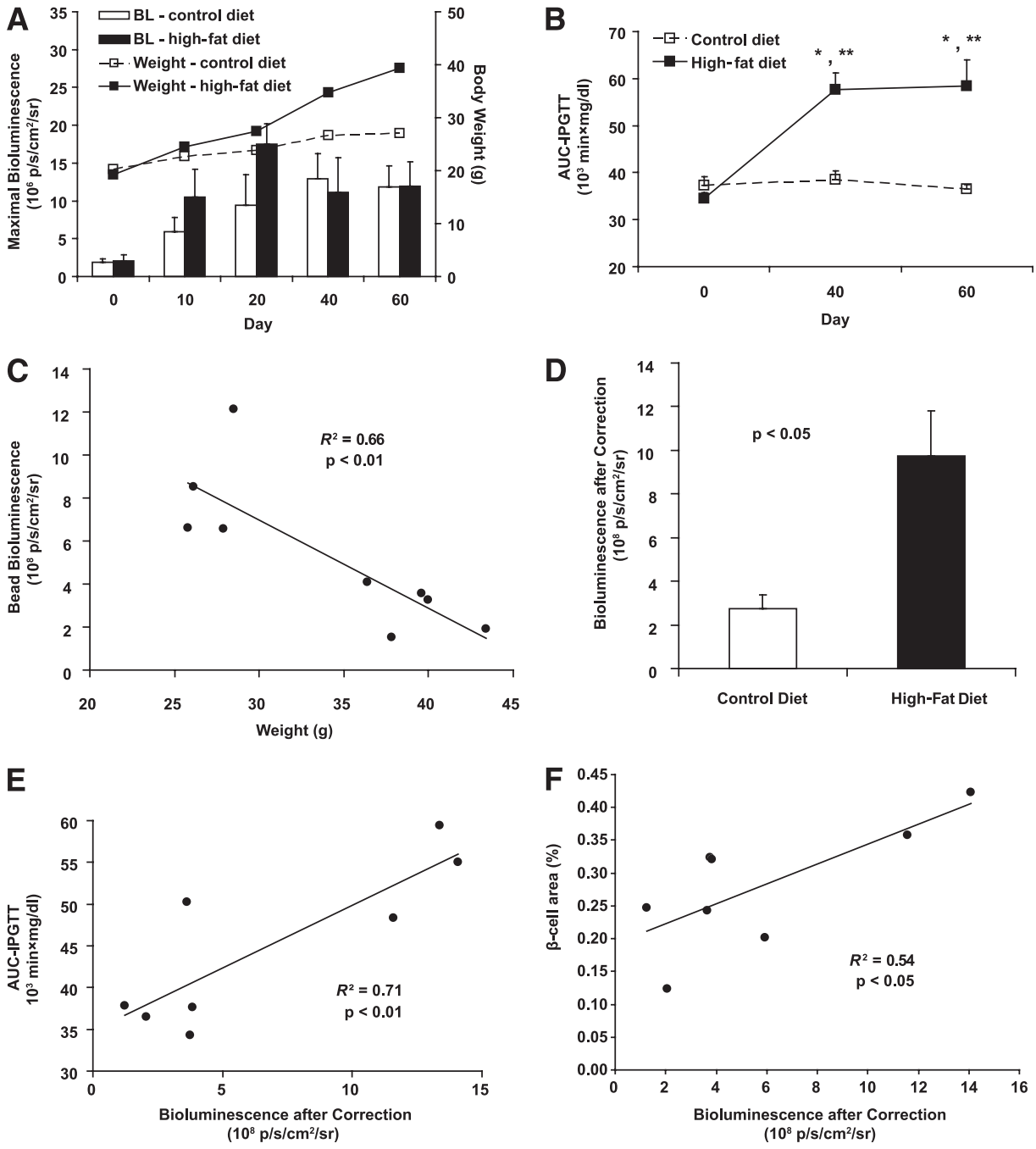

FIG. 5. CCD imaging of MIP-TF mice in the HFD model of type 2 diabetes. *A*: Longitudinal monitoring of pancreas region bioluminescence (BL) from MIP-TF mice fed a normal (white bar) or a HFD (black bar). Data shown are the mean maximum photons/seconds/squared centimeters/steradian ± SEM. Solid line indicates mean body weight ± SEM for MIP-TF mice fed a HFD; dashed line is that for control mice on a normal diet (n = 4 to 5 mice/group). *B*: Longitudinal monitoring of IPGTT in MIP-TF mice fed a HFD (solid line) or normal diet (dashed line). *$P < 0.05$ for HFD vs. normal diet at indicated time point by t test. ** $P < 0.05$ for HFD at indicated time point vs. the baseline at day 0 by t test. Bonferroni adjustment was applied for post hoc t test following repeated-measures ANOVA. *C*: Inverse correlation between MIP-TF mouse weight and the light detected from a luminescent bead placed on the pancreas. A luminescent bead that provides a constant light source was used to assess the extent to which obesity attenuated luminescence. Bead luminescence was inversely correlated with body weight (R^2 = 0.66 with $P < 0.01$). Individual mice are represented by black circles. *D*: After correction for reduced tissue transparency, bioluminescence from the pancreas region of HFD-fed mice (black bar) was an average of 3.6-fold higher than control mice (white bar) at day 60. Data shown are average ± SEM (n = 4 to 5 mice/group). $P < 0.05$ by two-tailed t test. *E*: AUC-IPGTT (obtained at day 60) was linearly correlated with bioluminescence after correction ($P < 0.01$). Individual mice are represented by black dots (n = 8). *F*: Data shown are pancreatic β-cell area vs. corrected bioluminescence for individual control and HFD-fed MIP-TF mice (n = 4 mice/group; $P < 0.05$).

from pancreas region. Because STZ administration is highly toxic to multiple organ systems, MIP-TF mice together with GCV treatment may provide a less toxic alternative to induce experimental type 1 diabetes. Potentially, this also provides a suicide gene system to specifically ablate β-cells arising from stem cell therapy using MIP-TF stem cells.

Hyperglycemia has been reported to induce proinsulin expression in the mouse liver and other organs (24). Tg(RIP-luc) mice that were rendered diabetic by STZ

administration robustly express luciferase in their liver, but the expression of proinsulin/insulin was not demonstrated at the protein level in their liver (23). Although our MIP-TF mice express approximately 20-fold higher levels of pancreatic luciferase activity compared with Tg(RIP-luc) mice, we never detected bioluminescent signals from diabetic MIP-TF mouse livers or from other organs, indicating that if hyperglycemia activates transgene expression in liver cells or in other organs, it occurs in rare cells, or at extremely low levels, in these mice.

We generated the MIP-TF mice in C57BL/6 background because this mouse strain provides a very useful model of early type 2 diabetes when placed on a HFD (28,32–34). MIP-TF mice displayed a rapid weight gain shortly after being placed on a HFD, as well as progressively impaired glucose tolerance and elevated fasting blood glucose levels, as expected. A prominent feature of this model is increased mesenteric adipose tissue (35), and this overlaying tissue can attenuate pancreatic bioluminescence. Using a constant fluorescent standard to quantify this attenuation (as described in [5,18]), we corrected the pancreatic bioluminescence based on the animal's weight and found that the pancreatic signals in MIP-TF mice were about 3.6-fold greater than that from MIP-TF mice on a normal diet. The corrected bioluminescence showed a significant correlation with pancreatic β-cell area for individual MIP-TF mice, again suggesting that noninvasive monitoring of *MIP-TF* gene expression by BLI can provide a biomarker of endogenous β-cell mass. The increased β-cell area in HFD-fed mice reflects, in large part, increased insulin resistance. Consistent with this, we observed that the corrected pancreatic bioluminescence signals from individual mice correlated with their AUC-IPGTT. Although CCD imaging in type 2 diabetes models may have to take into account changes in the animal's body weight, microPET detection of reporter gene expression is unaffected by tissue depth since high-energy γ-photons are much more tissue penetrating (8), and can be corrected for attenuation if needed, but microPET imaging is much more expensive.

In summary, we have generated transgenic MIP-TF C57BL/6 mice in which the β-cells express a fusion of three different imaging reporters. We have demonstrated imaging of MIP-TF pancreatic β-cells by fluorescent microscopy, BLI, and microPET. The MIP-TF mice enabled noninvasive monitoring of β-cells in models of type 1 diabetes and type 2 diabetes. We believe the MIP-TF mice can expedite studies in a broad range of diabetes research, including studies of β-cell development, diabetes pathogenesis, stem cell differentiation into β-cells, transdifferentiation, and islet survival after transplantation. We are currently breeding the *TF* gene into the NOD mouse background and hope to provide a new tool for studying β-cell loss and β-cell replication in the context of autoimmunity.

ACKNOWLEDGMENTS

This work was supported by funding from the Juvenile Diabetes Research Foundation (5-2007-547) and the National Institutes of Health (R21-DK-080461) to D.L.K., as well as by funds from The Brehm Coalition for Diabetes Research to M.A.A.

No potential conflicts of interest relevant to this article were reported.

J.Y. performed experiments, designed experiments, and wrote the manuscript. J.R., H.D., Y.L., B.M., Z.Z., L.H., and M.N. performed experiments. D.B.S. performed experiments, designed experiments, and wrote the manuscript. M.A.A., J.T., S.S.G., and D.L.K. designed experiments and wrote the manuscript.

The authors thank Drs. Alvin Powers and John Virostko, Vanderbilt University, Nashville, TN, Frezghi Habte, Stanford University, Palo Alto, CA, and members of the University of California, Los Angeles, Crump Institute for Molecular Imaging for their help and technical expertise. The authors thank Dr. Nagichettiar Satyamurthy and Waldemar Ladno, University of California, Los Angeles, CA, and Drs. David Dick and Fred Chin, Stanford University, Palo Alto, CA, for production of the PET tracers.

REFERENCES

1. Lu Y, Dang H, Middleton B, et al. Bioluminescent monitoring of islet graft survival after transplantation. Mol Ther 2004;9:428–435
2. Fowler M, Virostko J, Chen Z, et al. Assessment of pancreatic islet mass after islet transplantation using in vivo bioluminescence imaging. Transplantation 2005;79:768–776
3. Smith SJ, Zhang H, Clermont AO, et al. In vivo monitoring of pancreatic beta-cells in a transgenic mouse model. Mol Imaging 2006;5:65–75
4. Park SY, Wang X, Chen Z, et al. Optical imaging of pancreatic beta cells in living mice expressing a mouse insulin I promoter-firefly luciferase transgene. Genesis 2005;43:80–86
5. Virostko J, Radhika A, Poffenberger G, et al. Bioluminescence imaging in mouse models quantifies beta cell mass in the pancreas and after islet transplantation. Mol Imaging Biol 2010;12:42–53
6. Virostko J, Powers AC. Molecular imaging of the pancreas in small animal models. Gastroenterology 2009;136:407–409
7. Phelps ME. Positron emission tomography provides molecular imaging of biological processes. Proc Natl Acad Sci USA 2000;97:9226–9233
8. Massoud TF, Gambhir SS. Molecular imaging in living subjects: seeing fundamental biological processes in a new light. Genes Dev 2003;17:545–580
9. Lu Y, Dang H, Middleton B, et al. Long-term monitoring of transplanted islets using positron emission tomography. Mol Ther 2006;14:851–856
10. Kim SJ, Doudet DJ, Studenov AR, et al. Quantitative micro positron emission tomography (PET) imaging for the in vivo determination of pancreatic islet graft survival. Nat Med 2006;12:1423–1428
11. Lu Y, Dang H, Middleton B, et al. Noninvasive imaging of islet grafts using positron-emission tomography. Proc Natl Acad Sci USA 2006;103:11294–11299
12. Souza F, Simpson N, Raffo A, et al. Longitudinal noninvasive PET-based beta cell mass estimates in a spontaneous diabetes rat model. J Clin Invest 2006;116:1506–1513
13. Goland R, Freeby M, Parsey R, et al. ^{11}C-dihydrotetrabenazine PET of the pancreas in subjects with long-standing type 1 diabetes and in healthy controls. J Nucl Med 2009;50:382–389
14. McGirr R, Hu S, Yee SP, Kovacs MS, Lee TY, Dhanvantari S. Towards PET imaging of intact pancreatic Beta cell mass: a transgenic strategy. Mol Imaging Biol 6 October 2010 [Epub ahead of print]
15. Ray P, De A, Min JJ, Tsien RY, Gambhir SS. Imaging tri-fusion multimodality reporter gene expression in living subjects. Cancer Res 2004;64:1323–1330
16. Kim YJ, Dubey P, Ray P, Gambhir SS, Witte ON. Multimodality imaging of lymphocytic migration using lentiviral-based transduction of a tri-fusion reporter gene. Mol Imaging Biol 2004;6:331–340
17. Hara M, Yin D, Dizon RF, Shen J, Chong AS, Bindokas VP. A mouse model for studying intrahepatic islet transplantation. Transplantation 2004;78:615–618
18. Virostko J, Chen Z, Fowler M, Poffenberger G, Powers AC, Jansen ED. Factors influencing quantification of in vivo bioluminescence imaging: application to assessment of pancreatic islet transplants. Mol Imaging 2004;3:333–342
19. Deltour L, Leduque P, Blume N, et al. Differential expression of the two nonallelic proinsulin genes in the developing mouse embryo. Proc Natl Acad Sci USA 1993;90:527–531
20. Lamotte L, Jackerott M, Bucchini D, Jami J, Joshi RL, Deltour L. Knock-in of diphteria toxin A chain gene at Ins2 locus: effects on islet development and localization of Ins2 expression in the brain. Transgenic Res 2004;13:463–473
21. Pugliese A, Zeller M, Fernandez A Jr, et al. The insulin gene is transcribed in the human thymus and transcription levels correlated with allelic

variation at the INS VNTR-IDDM2 susceptibility locus for type 1 diabetes. Nat Genet 1997;15:293–297
22. Ben-Yehudah A, Reinhart B, Navara C, et al. Specific dynamic and non-invasive labeling of pancreatic beta cells in reporter mice. Genesis 2005;43:166–174
23. Chen X, Larson CS, West J, Zhang X, Kaufman DB. In vivo detection of extrapancreatic insulin gene expression in diabetic mice by bioluminescence imaging. PLoS ONE 2010;5:e9397
24. Kojima H, Fujimiya M, Matsumura K, Nakahara T, Hara M, Chan L. Extrapancreatic insulin-producing cells in multiple organs in diabetes. Proc Natl Acad Sci USA 2004;101:2458–2463
25. Bustos M, Sangro B, Alzuguren P, et al. Liver damage using suicide genes. A model for oval cell activation. Am J Pathol 2000;157:549–559
26. Ray P, De A, Patel M, Gambhir SS. Monitoring caspase-3 activation with a multimodality imaging sensor in living subjects. Clin Cancer Res 2008;14:5801–5809
27. Bonnevie-Nielsen V, Steffes MW, Lernmark A. A major loss in islet mass and B-cell function precedes hyperglycemia in mice given multiple low doses of streptozotocin. Diabetes 1981;30:424–429
28. Surwit RS, Kuhn CM, Cochrane C, McCubbin JA, Feinglos MN. Diet-induced type II diabetes in C57BL/6J mice. Diabetes 1988;37:1163–1167
29. Ahrén B, Simonsson E, Scheurink AJ, Mulder H, Myrsén U, Sundler F. Dissociated insulinotropic sensitivity to glucose and carbachol in high-fat diet-induced insulin resistance in C57BL/6J mice. Metabolism 1997;46:97–106
30. Hull RL, Kodama K, Utzschneider KM, Carr DB, Prigeon RL, Kahn SE. Dietary-fat-induced obesity in mice results in beta cell hyperplasia but not increased insulin release: evidence for specificity of impaired beta cell adaptation. Diabetologia 2005;48:1350–1358
31. O'Brien BA, Harmon BV, Cameron DP, Allan DJ. Beta-cell apoptosis is responsible for the development of IDDM in the multiple low-dose streptozotocin model. J Pathol 1996;178:176–181
32. Surwit RS, Feinglos MN, Rodin J, et al. Differential effects of fat and sucrose on the development of obesity and diabetes in C57BL/6J and A/J mice. Metabolism 1995;44:645–651
33. Fearnside JF, Dumas ME, Rothwell AR, et al. Phylometabonomic patterns of adaptation to high fat diet feeding in inbred mice. PLoS One 2008;3:e1668
34. Lin S, Thomas TC, Storlien LH, Huang XF. Development of high fat diet-induced obesity and leptin resistance in C57Bl/6J mice. Int J Obes Relat Metab Disord 2000;24:639–646
35. Rebuffé-Scrive M, Surwit R, Feinglos M, Kuhn C, Rodin J. Regional fat distribution and metabolism in a new mouse model (C57BL/6J) of non-insulin-dependent diabetes mellitus. Metabolism 1993;42:1405–1409